FINNISH METEOROLOGICAL INSTITUTE
CONTRIBUTIONS

NO. 71

EXPERIMENTAL STUDIES ON AEROSOL PHYSICAL PROPERTIES AND TRANSFORMATION IN ENVIRONMENTAL CHAMBERS

ARI LESKINEN

DEPARTMENT OF PHYSICS
UNIVERSITY OF KUOPIO
KUOPIO, FINLAND

DOCTORAL DISSERTATION

To be presented, with the permission of the Faculty of Natural and Environmental Sciences of the University of Kuopio for public examination in Auditorium L22, Snellmania building, University of Kuopio, on May 9th, 2008, at 1 p.m.

Finnish Meteorological Institute
Helsinki, 2008

ISBN 978-951-697-665-8 (paperback)
ISSN 0782-6117

Yliopistopaino
Helsinki, 2008

FINNISH METEOROLOGICAL INSTITUTE

Published by Finnish Meteorological Institute
Erik Palménin aukio 1, P.O. Box 503
FI-00101 Helsinki, Finland

Series title, number and report code of publication
Contributions 71, FMI-CONT-71

Date
April 2008

Author
Ari Leskinen

Name of project

Commissioned by

Title
EXPERIMENTAL STUDIES ON AEROSOL PHYSICAL PROPERTIES AND TRANSFORMATION IN ENVIRONMENTAL CHAMBERS

Abstract

Aerosol particles in the atmosphere are known to influence the atmosphere's radiation balance by scattering sunlight and acting as condensation nuclei for reflective clouds. The particles are also known to possess negative health effects, since they may carry harmful compounds deep into the lungs. Aerosols are emitted from both natural and anthropogenic sources, such as combustion. Usually, the emissions at their sources are well known, but the behavior of emissions in the atmosphere needs to be further investigated, since the particles may undergo considerable changes in their composition and properties during their lifetime in the atmosphere.

This thesis presents experimental studies on different kinds of aerosols, their formation and aging. The examined aerosols were wood chip combustion aerosol, diesel engine exhaust, and mineral and metal dusts, and they were characterized according to their particle size distribution, volatility at different temperatures and organic carbon content. The emissions from wood combustion and a diesel power aggregate were also monitored overnight in an environmental chamber in order to find out the changes in the properties during aging.

The geometric mean diameter of the particles from the combustion sources was found to be 63-115 nm, depending on the combustion conditions, engine type, speed and load, and fuel. The volatile fraction of the apparent volume of the freshly emitted particles at a temperature of 360 °C was found to be 20-32 % for wood combustion particles and 37-45 % for diesel particles. Both the geometric mean diameter and the volatility of the particles were observed to increase with aging. For wood combustion particles, the contribution of coagulation to particle growth was found to be higher than for the diesel engine exhaust particles. In the aging experiments also new particles were observed to form in the chamber. These particles were found to be almost completely (98-99 %) volatile. The new particle formation was also studied by conducting photooxidation experiments with xylene and nitrogen dioxide in an indoor smog chamber. In these experiments, intensive particle formation and fast subsequent growth was observed. From the experimental data, the concentration of condensable vapors was estimated by applying the concept of condensation sink, previously applied to atmospheric measurements. The vapor concentrations were found to be remarkably higher in the chamber than, on average, in the atmosphere. The high values in the chamber were observed to be the same magnitude as those observed in a highly polluted area.

The experiments in this thesis showed that the aging of combustion derived aerosols in the atmosphere can be simulated in environmental chambers. However, the processes in environmental chambers may overestimate the processes in the atmosphere due to higher concentrations of injected compounds or aerosols and more intensive UV radiation, and also experiments with lower concentrations and UV levels should be conducted in order to get more comparable results. The experiments also show that the volatility tandem differential analysis is a relevant on-line method for estimating the organic fraction of aerosol particles. This agreement was found qualitative in the aging experiments and quantitative in the passenger car exhaust experiments. In order to better the time resolution of the particle volatility measurements, a set-up with several preset temperatures should be used.

Publishing unit
Finnish Meteorological Institute, Research and Development, Kuopio Unit

Classification (UDC)
541.182.2/.3, 53.083, 662.613

Keywords
Aerosols, Aging, Measurements

ISSN and series title
0782-6117 Finnish Meteorological Institute Contributions

ISBN
978-951-697-665-8

Language
English

Sold by
Finnish Meteorological Institute / Library
P.O. Box 503, FI-00101 Helsinki
Finland

Pages
116

Price

Note

ILMATIETEEN LAITOS

Julkaisun sarja, numero ja raporttikoodi
Contributions 71, FMI-CONT-71

Julkaisija Ilmatieteen laitos, Erik Palménin aukio 1
PL 503, 00101 Helsinki

Julkaisuaika
Huhtikuu 2008

Tekijä(t)
Ari Leskinen

Projektin nimi

Toimeksiantaja

Nimeke
AEROSOLIEN FYSIKAALISET OMINAISUUDET JA MUUTUNTAKOKEET YMPÄRISTÖKAMMIOISSA

Tiivistelmä

Ilmakehän aerosolihiukkasten tiedetään vaikuttavan mm. ilmakehän säteilytasapainoon sirottamalla säteilyä (suora vaikutus) ja toimimalla tiivistymisytiminä pilvipisaroille, jotka heijastavat säteilyä (epäsuora vaikutus). Pienhiukkasilla on todettu myös haitallisia terveysvaikutuksia, koska ne kulkeutuvat helposti hengityselimistöön ja kuljettavat sinne haitallisia yhdisteitä. Ilmakehän hiukkaset ovat sekä luontoperäisiä että ihmisen toiminnan, kuten polttoprosessien, sinne tuottamia. Eri lähteiden tuottamia hiukkasia on tutkittu paljon, mutta myös niiden käyttäytymistä ilmakehässä tulisi seurata, koska päästöhiukkasten koostumuksessa ja ominaisuuksissa voi tapahtua huomattaviakin muutoksia niiden olinaikana ilmakehässä.

Tässä väitöskirjassa esitetään kokeellisia tutkimustuloksia erilaisista aerosoleista, niiden muodostumisesta ja ikääntymisestä. Tutkitut aerosolit olivat peräisin puuhakkeen poltosta, dieselkäyttöisistä moottoreista (aggregaatti ja henkilöautot) ja mineraali- ja metallipölyjen tuotosta ja niitä karakterisoitiin hiukkaskokojakauman, haihtuvuuden ja hiilisisällön perusteella. Puunpolton ja dieselaggregaatin päästöjä myös seurattiin vuorokauden ajan ulkona sijaitsevassa ympäristökammiossa muutosten selvittämiseksi hiukkasten kokojakaumassa, haihtuvuudessa ja hiilisisällössä.

Puunpolton hiukkasten koon (geometrinen keskihalkaisija) havaittiin olevan 72-86 nm, dieselaggregaatin päästöhiukkasten koon 66-85 nm ja dieselkäyttöisten henkilöautojen päästöhiukkasten koon 63-115 nm. Tuotettujen hiukkasten kokoon vaikuttivat palamisolot, moottorin tyyppi, käyntinopeus ja kuorma, sekä polttoaine. Tuoreiden puunpolton hiukkasten tilavuudesta 20-32 % oli haihtuvaa ja dieselaggregaatin päästöhiukkasten tilavuudesta 37-45 %. Sekä hiukkasten koon että haihtuvuuden todettiin kasvavan ikääntymisen myötä. Hiukkasia kasvattavan koagulaation osuuden havaittiin olevan suurempi puunpolton hiukkasille kuin dieselaggregaatin päästön hiukkasille. Ikääntymiskokeissa kammiossa havaittiin myös uusien hiukkasten muodostumista. Näiden hiukkasten havaittiin olevan lähes kokonaan (98-99 %) haihtuvia. Tutkittaessa uusien hiukkasten muodostumista myös sisätiloissa olevassa kammiossa säteilyttämällä UV-valolla ksyleenin ja typenoksidien seosta havaittiin voimakasta hiukkasmuodostusta ja nopeaa hiukkasten kasvua. Kokeellisista tuloksista arvioitiin kammiossa olleiden tiivistymiskykyisten höyryjen pitoisuutta, joiden havaittiin olevan huomattavasti suuremmat kuin keskimäärin ilmakehässä ja vastaavan erittäin saastuneilla alueilla havaittuja arvoja.

Tähän väitöskirjaan liittyvissä kokeissa todennettiin, että ilmakehässä tapahtuvia aerosoliprosesseja voidaan simuloida ympäristökammioissa, vaikkakin aerosoliprosessit kammioissa saattavat yliarvioida aerosoliprosesseja ilmakehässä, koska kammiokokeissa helposti syötetään korkeampia lähtöaineiden pitoisuuksia ja käytetään voimakkaampaa UV-säteilyä kuin ilmakehässä. Kammiokokeissa havaittiin, että käytetty suoraan osoittava menetelmä antoi kvalitatiivisesti samansuuntaisia tuloksia kuin keräykseen ja jälkeenpäin tehtävään analyysiin perustuva orgaanisen fraktion määritys. Dieselkäyttöisten henkilöautojen päästötutkimuksessa näiden analyysien välillä todettiin myös kvantitatiivinen yhteys. Käytetyn haihtuvuusmittauksen aikaresoluutio oli kuitenkin heikko ja tarkempaa aikaresoluutiota vaativissa mittauksissa kannattaakin käyttää järjestelyä, jossa näyte voidaan lämmittää nopeasti eri lämpötiloihin.

Julkaisijayksikkö
Kuopion yksikkö

Luokitus (UDK)
541.182.2/.3, 53.083, 662.613

Asiasanat
aerosoli, ikääntyminen, mittausmenetelmät

ISSN ja avainnimike
0782-6117 Finnish Meteorological Institute Contributions

ISBN
978-951-697-665-8

Kieli
englanti

Myynti
Ilmatieteen laitos / Kirjasto
PL 503, 00101 Helsinki

Sivumäärä
116

Hinta

Lisätietoja

ACKNOWLEDGMENTS

The work presented in this thesis has been carried out at the Department of Environmental Science, Univ. Kuopio (UKU), and at the Kuopio Unit of Finnish Meteorological Institute (FMI), during the period 1998-2008. I am grateful to both institutes for providing the working facilities.

I gratefully thank my principal supervisor, Prof. Kari Lehtinen, head of the FMI's Kuopio Unit, for employing me at FMI in 2005 and for guiding me with excellence to complete this work. I also thank my other supervisor, Prof. Jorma Jokiniemi, head of the Fine Particle and Aerosol Technology Laboratory at UKU, for guidance.

I also think back with gratitude and respect to Prof. Taisto Raunemaa (1939–2006), who in 1997, as then the head of the Laboratory for Atmospheric Physics and Chemistry at UKU, employed me for the research projects this thesis is based on and acted as my first supervisor.

I also wish to thank the preliminary examiners, Prof. Kaarle Hämeri, Univ. of Helsinki (UHEL), and Prof. Veli-Matti Kerminen, FMI, for critically reviewing this thesis and for their valuable comments.

I would like to thank all my co-authors, at FMI, UKU, UHEL and the Finnish Institute of Occupational Health. It has been a great pleasure to work together.

My thanks also go to the former co-workers at the Laboratory for Atmospheric Chemistry ("IFK"), as well as to the members of FMI's Kuopio unit, my current group. The humorous atmosphere has made very many days of ours, let's just keep it up!

I also want to thank numerous colleagues and friends for giving me support and hints, how to continue this work when my own head has felt like a total vacuum, and for giving me – sometimes quite spontaneous – opportunities to think about totally something else than this work.

Finally, my warmest thanks go to my wife Anu and my daughter Aada for their love and understanding, especially during these years I've been writing this thesis. Dear Aada, I'm very glad to say that Isi has now finally "colored his coloring book".

Kuopio, April 2008

Ari Leskinen

CONTENTS

LIST OF ORIGINAL PUBLICATIONS

This thesis consists of an Introduction and five original papers:

Paper I: Leskinen, A. P., Jokiniemi, J. K. and Lehtinen, K. E. J., Characterization of aging wood chip combustion aerosol in an environmental chamber, *Atmos. Environ.*, **41**, 3713-3721, doi:10.1016/j.atmosenv.2006.12.016, 2007.

Paper II: Leskinen, A. P., Jokiniemi, J. K. and Lehtinen, K. E. J., Transformation of diesel engine exhaust in an environmental chamber, *Atmos. Environ.*, **41**, 8865-8873, doi:10.1016/j.atmosenv.2007.08.021, 2007.

Paper III: Leskinen, A., Kulmala, M. and Lehtinen, K. E. J., Growth of nucleation mode particles: source rates of condensable vapour in a smog chamber, *Atmos. Environ.*, **Under review**, 2008.

Paper IV: Linnainmaa, M., Laitinen, J., Leskinen, A., Sippula, O., and Kalliokoski, P., Laboratory and field testing of sampling methods for inhalable and respirable dust, *J. Occup. Hygiene*, **5**, 28-35, doi:10.1080/15459620701763723, 2008.

Paper V: Ålander, T. J. A., Leskinen, A. P., Raunemaa, T. M., and Rantanen, L., Characterization of diesel particles: Effects of fuel reformulation, exhaust aftertreatment, and engine operation on particle carbon composition and volatility, *Environ. Sci. Technol.*, **38**, 2707-2714, doi:10.1021/es030129j, 2004.

A. Leskinen is responsible for the major work as well as for the manuscript writing in Papers I, II and III. In Paper IV A. Leskinen is responsible for the dust generation system development and use, for particle penetration test system development and tests together with O. Sippula, for measurement and analysis of particle size distribution in the environmental chamber, and for related writing of the manuscript. In Paper V A. Leskinen is responsible for the particle size distribution and volatility measurements and development of the applied measurement method (volatility tandem differential analyzer) and its data analysis.

1 INTRODUCTION

The recent changes in the atmosphere are partly due to anthropogenic activities, such as combustion of fossil fuels. Scenarios of long-term effects on the global change in the atmosphere suggest e.g. rise of the average temperature by several degrees Celsius and enhancement of ultraviolet (UV) radiation in the lower atmosphere due to ozone depletion in the upper atmosphere. Aerosol particles suppress the temperature rise by scattering incoming solar radiation back to space and by acting as condensation nuclei for cloud droplets, which increase the albedo of the atmosphere [*IPCC*, 2007]. The particles are also reported to possess negative health effects [e.g. *Pope and Dockery*, 2006], because they penetrate deep into the lungs and may carry harmful compounds.

In deepening the knowledge of the aerosol effects in the atmosphere and on e.g. human health, knowing the properties of aerosols from different emission sources is essential. Also more knowledge on the aging of primary emission and formation of secondary products in the atmosphere are needed. The aerosols emitted directly from the sources or suspended in the air can be analyzed from stack or exhaust pipe, or at atmospheric measurement stations. The influence of different burner or engine types, fuels and loads on emissions can be studied in combustion laboratories or in vehicle emission laboratories equipped with a dynamometer. Furthermore, the aging of particles in the atmosphere can be studied by monitoring the emission e.g. by aircraft or balloon measurements, by taking samples at different points along the emission trajectory [*Hughes et al.*, 2000], or in controlled conditions in environmental chambers, as in this work. Environmental chambers have been earlier used e.g. in studies of diesel soot particles [*Strommen and Kamens*, 1999] and wood combustion aerosols [*Kamens et al.*, 1984]. Also pure organic compounds and their photooxidation have been studied in smog chambers [e.g. *Robinson et al.*, 2007]. Furthermore, in large environmental chambers, several aerosol measurement and sample collection devices can be tested in the same, usually predefined, conditions and aerosol concentrations simultaneously. In such experiments, e.g. the effect of varying concentration and aerosol load on the behavior of instruments can be studied in detail.

In this work, different kinds of aerosols, their formation and aging were studied. The main objectives of this work were to

- characterize the particles emitted by a domestic wood combustion boiler, a diesel-powered off-road engine and two types of diesel-fueled passenger cars, and those suspended in the air of a talc production plant, a metal smelter, and a metal foundry, based on their size distribution, number concentration, and volatility,

- find out the changes in the particle size distribution, concentration, volatility, and organic carbon fraction of wood combustion emissions and diesel engine exhaust after their release into the atmosphere during the next 24 hours,

- verify new particle formation and subsequent growth under controlled photooxi-

dation of an organic compound and nitrogen oxides, and find out the source rates of condensable vapors contributing to the particle growth with different concentrations of the ingredients.

Related to these objectives, the answers to the following specific questions were searched:

1. Is the volatility tandem differential analysis (VTDMA) a relevant on-line method for estimating the organic fraction of aerosol particles, at least qualitatively?
2. Do the aging of wood combustion aerosol and diesel engine exhaust differ from each other?
3. How do the aerosol processes in environmental chambers compare to the processes in the atmosphere?

2 THEORETICAL CONCEPTS

2.1 BASICS ON AEROSOLS

An *aerosol* is defined as a suspension of fine solid or liquid particles in a gas [e.g. *Hinds*, 1998]. In some contexts the term aerosol may refer to the particle phase only. However, in this thesis it refers to both the gas and particle phases. Furthermore, the gas phase refers to *air*, which is a mixture of nitrogen (N_2), oxygen (O_2), Argon (Ar) and numerous trace gases. Typically air also contains vapors, such as water and organic compounds. The concentration of the vapors in the air depends on the prevailing temperature and pressure and on the physico-chemical properties of the component, such as the vapor pressure.

Aerosol particles in the atmosphere originate from natural sources (e.g. wind blown dust, sea spray, volcanoes and plants) and from anthropogenic sources (e.g. fuel combustion) [e.g. *Seinfeld and Pandis*, 2006]. Aerosol components formed within a source and emitted directly into the atmosphere are called *primary aerosol components*, whereas those formed in the atmosphere by gas-to-particle conversion, either homogeneous or heterogeneous, are called *secondary aerosol components*. Aging of the particles may lead to the formation of multiple generations of secondary components. Furthermore, aged primary aerosol particles can contain secondary components and secondary aerosol particles can contain primary components via coagulation of the original primary particles and the secondary particles [*Fuzzi et al.*, 2006].

Aerosol components, such as organic compounds, fall into different categories depending on their phase of existence in the atmosphere. *Volatile* components have low molecular weights (carbon number less than five) and high vapor pressures and exist at tropospheric conditions exclusively in the gas phase of a system. Components with higher molecular weights can partition between gas and particle phases, depending on their vapor pressure and are called *semi-volatile* components. Some components exist almost exclusively in the (condensed) particulate phase and are therefore called *non-volatile* components [*Fuzzi et al.*, 2006].

When aerosol particles are concerned, their *size* usually refers to the diameter or equivalent diameter of the particle. The size of aerosol particles ranges from approximately 2 nm (1 nm $= 10^{-9}$ m) to approximately 100 μm (1 μm $= 10^{-6}$ m). The diameter is unambiguous for liquid droplets, but for solid particles the diameter cannot usually be measured directly and unambiguously. Generally, atmospheric particles are non-spherical with an unknown shape and density, and for them, a series of equivalent diameters have been introduced in the literature [e.g. *Hinds*, 1998]. The most important of these from the point of this thesis is the *electrical mobility equivalent diameter*, as the particle measurements have been carried out by using a differential mobility analyzer which classifies the particles according to their electrical mobility. The (electrical) mobility equivalent diameter, d_b, is the diameter of a spherical particle of unit density ($\rho_0 = 1000$ kg/m^3) having the same (electrical) mobility as the given particle. Other

important equivalent diameters are e.g. the *aerodynamic diameter*, d_{a}, the diameter of a unit density sphere having the same terminal settling velocity as the particle, and the *Stokes diameter*, d_{St}, the diameter of a sphere having the same terminal settling velocity and density as the particle. It is worth noticing that if the particle is spherical, the Stokes diameter equals the actual physical diameter.

The amount of particles is often characterized by the particle concentration, i.e. the amount of particles per unit volume of air. The most usual are number, surface area, volume and mass concentration, of which the most important are the number concentration (e.g. particles/m^3, particles/cm^3) and the mass concentration (e.g. mg/m^3, μg/m^3). In this thesis, the number concentration is under inspection almost exclusively.

A *monodisperse* aerosol contains particles that are all of the same size. This is, in practice, never the case in the atmosphere, but is rather connected to test aerosol production in the laboratory. The aerosol in the atmosphere is generally *polydisperse* with statistical measures, such as the number of modes (size categories) and their relative intensities, geometric mean diameters and geometric standard deviations, which characterize the aerosol over the particle size range in an easily representative way.

The size distribution of polydisperse aerosol particles is usually described by a log-normal distribution in which the logarithm of particle size is normally distributed. For a log-normal size distribution, the number concentration of particles having diameters whose logarithms are between $\ln d_{\mathrm{p}}$ and $\ln d_{\mathrm{p}} + d \ln d_{\mathrm{p}}$ is given as [*Hinds*, 1998]

$$dN = \frac{N}{\sqrt{2\pi} \ln \sigma_{\mathrm{g}}} \exp\left[-\frac{\left(\ln d_{\mathrm{p}} - \ln d_{\mathrm{g}}\right)^2}{2\left(\ln \sigma_{\mathrm{g}}\right)^2} \right] d \ln d_{\mathrm{p}}, \tag{2.1}$$

where N (cm^{-3}) is the number concentration, d_{g} is the geometric mean diameter, and σ_{g} is the geometric standard deviation. For ambient aerosols the size distribution is often described as the sum of n log-normal distributions, where n is the number of modes.

The geometric mean diameter in Equation (2.1) can be calculated, in discrete situation, from the data obtained with an aerosol instrument, by

$$d_{\mathrm{g}} = \exp\left[\frac{\sum_{i=1}^{j} \left(\ln d_{\mathrm{p},i}\right) \Delta N_i}{\sum_{i=1}^{j} \Delta N_i} \right], \tag{2.2}$$

where j is the number of size channels, $d_{\mathrm{p},i} = (d_{\mathrm{l},i} d_{\mathrm{u},i})^{1/2}$ is the geometric mean diameter of each size channel i, expressed as the geometric mean of the lower and upper cut sizes, $d_{\mathrm{l},i}$ and $d_{\mathrm{u},i}$, of the channel i, and ΔN_i is the number concentration of particles in size channel i.

The particle size of 2.5 μm is often used to divide particles into two modes: *fine particles* (diameter less than 2.5 μm) and *coarse particles*. In some occasions, supermicron particles (diameter more than 1 μm) are classified into the coarse particle fraction. In general, the origin and behavior of these modes differ from each other, and the distinction into these two modes is justified by the underlying physical properties of the

particles. Particles smaller than 0.1 μm in diameter are called *ultrafine particles*. In the atmosphere this ultrafine particle fraction contains most of the particles by number. The smallest ultrafine particles (below 20–25 nm) are called the *nucleation mode*. The nucleation mode particles are formed via hot vapor condensation in combustion processes, and via different mechanisms in atmospheric nucleation. The larger ultrafine particles (20–100 nm) are often called the *Aitken mode*. Particles in the size range of $\sim$0.1–1 μm are called the *accumulation mode*. The accumulation mode usually contains most of the surface area of a particle population and is important e.g. for heterogeneous reactions occurring on the surfaces of the particles. The source of the accumulation mode is coagulation and growth by condensation of the nuclei mode particles. The removal mechanisms are the weakest for accumulation mode particles, and particles tend to accumulate into this size class, hence the name accumulation mode [*Seinfeld and Pandis*, 2006].

2.2 Condensation and evaporation

In *condensation* vapor is transferred from the gas phase to the particulate phase and in *evaporation* vice versa. Both processes change the particle diameter and the size distribution of the particle population. The driving force for both condensation and evaporation for a given compound arises from the difference between the vapor pressure of the compound far from the particles (p_i) and the equilibrium vapor pressure ($p_{\mathrm{eq},i}$). The particle growth rate associated with condensation/evaporation can be expressed as [*Seinfeld and Pandis*, 2006]

$$\frac{dd_{\mathrm{p}}}{dt} = \frac{4D_i M_i}{RTd_{\mathrm{p}}\rho_{\mathrm{p}}} f(Kn,\alpha)\left(p_i - p_{\mathrm{eq},i}\right), \tag{2.3}$$

where D_i is the diffusivity for compound i in air (m^{2}s^{-1}), M_i is its molecular weight (kg/mol), $R = 8.3145$ J/(molK) is the ideal gas law constant, T is temperature (K), ρ_{p} is the particl density (kg/m^3), and $f(Kn,\alpha)$ is the correction due to non-continuum effects and imperfect surface accommodation, characterized by the Knudsen number, Kn, and the accommodation coefficient, α. For condensation the growth rate given by Equation (2.3) is positive and for evaporation negative.

2.3 Coagulation

Aerosol particle coagulation arises from aerosol particles coming into contact with each other because of the difference in their relative motion. The particles may collide due to their thermal (Brownian) motion, or due to motion caused by external forces, such as electrical or gravitational forces. Opposite to the elastic collision between gas molecules, the aerosol particles usually collide inelastically and stay in contact. Usually the sticking probability of the two colliding particles is assumed to equal unity.

The coagulation rate depends on the particle number concentration and the difference in particle size. The coagulation rate is lowest when the two particles are of the same size, and increases when the difference in particle size increases. This phenomenon can be explained in the following way. The larger and slower particle provides a large surface area for the smaller and faster particles for deposition. Collisions between two large particles happen slowly because of their slow speed. Small particles move fast, but miss each other because of their small collision areas.

For an approximately monodisperse aerosol population the size and number concentration change rates due to coagulation can be expressed, assuming that the volume fraction of particulate matter in the aerosol population is conserved and that the particles are spherical, as

$$\frac{dd_{\mathrm{p}}}{dt} = \frac{1}{6} K N d_{\mathrm{p}}, \tag{2.4}$$

and

$$\frac{dN}{dt} = -\frac{1}{2} K N^2, \tag{2.5}$$

where K is the coagulation coefficient, N is the particle number concentration (cm^{-3}) and d_{p} is the particle diameter, i.e. the geometric mean diameter for the aerosol population. From Equations (2.4) and (2.5) one can see that the particle size increases and the number concentration decreases as the coagulation proceeds. For the coagulation coefficient, a value of K $\approx$1–2$\times 10^{-9}$ $\mathrm{cm}^3\mathrm{s}^{-1}$ is applicable for a wide size range for nearly monodisperse aerosol populations [*Hinds*, 1998].

2.4 NUCLEATION

At suitable conditions, new particles can form from non- or low-volatile gaseous precursors via a process called nucleation, which is known to occur in the atmosphere and in combustion. Usually, the exact nucleation mechanism is not known [e.g. *Holmes*, 2007]. Proposed nucleation mechanisms in the literature are e.g. kinetic "coagulation" [*Girshick and Chiu*, 1990], binary (sulphuric acid and water) [*Kulmala and Laaksonen*, 1990], ternary (sulphuric acid–ammonia–water) [*Korhonen et al.*, 1999], ion-induced [*Lee et al.*, 2003] and activation of existing clusters [*Kulmala et al.*, 2007a, 2006] in atmospheric nucleation, and condensation of the oxidation and/or pyrolysis products of fuel molecules in combustion [*Haynes and Wagner*, 1981].

New particle formation in the atmosphere, i.e. nucleation and growth to detectable sizes, has been detected qualitatively in as early as the 1890s by Aitken. During the recent decades also quantitative analysis has become possible owing to the development of measurement instruments that are capable of measuring down to 3 nm sized particles [*McMurry*, 2000] and even below 2 nm for suitable material, such as sodium chloride [*Mordas et al.*, 2008]. Particle formation has been detected in a variety of locations and environments all over the world, and over different time periods [*Kulmala et al.*, 2004], as well as in laboratory experiments in environmental chambers [e.g. *Stern et al.*,

1987]. The majority of the atmospheric observations have been made at fixed sampling points, which enables long-time measurements. Aircraft or ship measurements have been carried out in investigation of the moving air parcel. The aircraft measurements require fast measurement instruments, ones with typical response times of the order of 1 s, which can be attained e.g. by using a condensation particle counter battery presented by *Kulmala et al.* [2007b].

The main species believed to be taking part in the atmospheric nucleation process are the above mentioned sulphuric acid and ammonia. Organic vapors have been proposed to contribute very little to particle nucleation but they contribute predominantly to the growth of the newly formed particles together with sulfuric acid (more effective up to around 10–20 nm size) [*Wehner et al.*, 2005]. The particle growth may also be contributed by the growth of the non-volatile core material, which affects the volatility of the particles [*Ehn et al.*, 2007; *Wehner et al.*, 2005]. The particles can grow further to the size of cloud condensation nuclei, which makes nucleation an important factor e.g. for global climate change models.

2.5 HETEROGENEOUS REACTIONS

Particles in the atmosphere also serve as active reaction sites for chemical (heterogeneous) reactions, which influence the partitioning of semi-volatile compounds between the gas and particle phases, as the reactants and the reaction products usually have different vapor pressures. For example, oligomers or polymers with low vapor pressures may be formed and partitioned into the particle phase in the reactions of two or more monomers that alone would be partitioned into the gas phase [*Vesterinen et al.*, 2007]. This polymerization is a long-term process that can last over more than 20 h [*Kalberer et al.*, 2004] and it can follow e.g. from acid-catalyzed (mainly sulfuric and nitric acid) particle-phase reactions of atmospheric carbonyls and hydrates [*Jang et al.*, 2002].

Also anthropogenic pollutants in the gas phase, such as SO_2, NO_x and NH_3 may react with primary aerosol particles, resulting in e.g. formation of sulfates and nitrates in the particles, such as aged sea-salt and mineral aerosols [*Song and Carmichael*, 1999]. The mineral dust particles may also affect the photochemical oxidant cycles by interacting with the radicals formed in the photochemical reactions [*Dentener et al.*, 1996].

2.6 CLOUD PROCESSING

Cloud processing, i.e. activation into a cloud droplet and subsequent evaporation of the cloud water, can also change the particle composition. For example, gaseous SO_2 can become oxidized in the liquid phase of the activated particles into sulfate, which remains in the particle phase even if the water evaporates. This in-cloud sulfate production increases the dry particle size and has been observed to occur in clouds in the atmosphere by *Wang et al.* [2007].

3 METHODS AND EXPERIMENTAL SETUPS

3.1 APPLIED ANALYTICAL METHODS

3.1.1 On-line particle analyses

3.1.1.1 Scanning mobility particle sizer (SMPS)

The particle size distributions in the aerosol aging and passenger car exhaust experiments [Paper I, Paper II, Paper III, Paper V] were measured with a scanning mobility particle sizer (SMPS) [*Wang and Flagan*, 1990]. An SMPS consists of a differential mobility analyzer (DMA) [*Knutson and Whitby*, 1975], which classifies particles into narrow size channels based on their electrical mobility, a condensation particle counter (CPC), which measures the number concentration of the classified particles, and software, which controls the operation of the DMA and CPC. In the SMPS system the particle size distribution is measured by scanning the DMA's central rod potential from the lower end to the upper end, and by measuring simultaneously the particle concentration continuously. With help of a computer software, the size distribution can be inverted from the data as the measurement proceeds.

Before the DMA the polydisperse particle sample is first charged with a radioactive Kr-85 neutralizer into an equilibrium charge distribution [*Wiedensohler*, 1988]. The charge distribution is bipolar and depends on particle size. The fraction of negatively charged particles is slightly larger than that of positively charged particles. Some particles are able to carry more than one elementary charge and are therefore called multiply charged particles.

The charged sample is introduced in an annular flow into the heart of the DMA, the classifying tube, which consists of an earthed outer electrode and a high voltage central electrode. In the beginning of the classifying tube, the aerosol flows in the vicinity of the outer electrode in a thin layer, and is separated from the central electrode by a sheath air flow. Between the two electrodes a nearly uniform radial electric field is developed. As the particles enter the electric field, negatively charged particles are collected on the outer electrode surface. Neutral particles carry on their straightforward movement in the aerosol flow and positively charged particles penetrate through the sheath air flow towards the central electrode. In the end of the central electrode, a selected fraction of the particles exits through a narrow slit as quasi-monodisperse aerosol. The quasi-monodisperse aerosol particles possess a certain electric mobility, which is determined by the flow rates in the classifying tube and the by central electrode potential. As electric mobility is a function of both particle size and charge, not all the particles are of the same size. Roughly, the diameter of the multiply charged (n elementary charges) particles is n times that of the singly charged particles. The appearance of multiply charged particles must be taken into account when size dependent parameters are measured. In size distribution measurements with an SMPS system this is normally

handled by the software.

From the DMA, the quasi-monodisperse aerosol is transported to the CPC, in which the working fluid can be butanol or water [*Hering et al.*, 2005]. In this thesis, butanol-based CPCs were used. In a butanol-based CPC, the sample flows first through a saturator, where liquid butanol is heated in order to produce butanol vapor. The vapor then mixes with the colder sample, and the particles and the vapor move along into a condenser tube, where the vapor quickly condenses on the particles and the particles grow. The grown particles move further into the optics where they are detected by a laser beam. A CPC is capable of calculating the particles one by one when the particle concentration is low (e.g. for TSI Model 3022A less than 10^4 cm^{-3}). At higher concentrations the resolution of the optics will be suffered by a coincidence phenomenon, i.e. multiple particles are detected as one particle. The correction for the coincidence can be and usually is included in the CPC's memory program.

The particle concentration limits vary from CPC model to another. The detection size limits depend on the temperature difference between the saturator and the condenser, which is factory set to a certain value. For example, for TSI Model 3022A the concentration range and factory set lower detection limit are 0–10^7 cm^{-3} and 7 nm (50 % detection efficiency), and for TSI Model 3025A 0–10^5 cm^{-3} and 3 nm, respectively. In both CPCs the upper detection limit is approximately 10 μm. By increasing the temperature difference, even smaller particles, down to a limit specific to the CPC model, can be detected.

In this thesis only the submicrometer particle size range was inspected. In the outdoor chamber experiments [Paper I, Paper II], two SMPS systems were used in parallel. The measured size (mobility equivalent diameter) ranges for the SMPS systems were 3–75 nm (TSI Model 3085 DMA and Model 3025A CPC) and 14–777 nm (TSI Model 3071 DMA and Model 3022A CPC). In the overlapping size region of 14–75 nm the data from the latter SMPS were used. The sheath air and aerosol volumetric flow rates were 10 l/min and 0.3 l/min or 7.5 l/min and 1.5 l/min for the Model 3085 DMA and 3.0 l/min and 0.3 l/min for the Model 3071 DMA, respectively. In the indoor smog chamber experiments [Paper III] the TSI Model 3071 DMA and Model 3022A pair was used with sheath air and aerosol flows of 10 l/min and 1.0 l/min, respectively, in the size range of 7–330 nm. In the passenger car exhaust measurements [Paper V] with the same DMA-CPC pair the values were 6.0 l/min for sheath air flow, 0.6 l/min for aerosol flow, and 10–480 nm for the size range.

3.1.1.2 Volatility tandem differential mobility analyzer (VTDMA)

A tandem differential mobility analyzer (TDMA) technique [*Rader and McMurry*, 1986] can be used to study various properties of (quasi-)monodisperse aerosols. The TDMA consists of a classifying DMA, which selects a quasi-monodisperse fraction of known size, a conditioning device, which alters the particles or the environment, and a scanning DMA and particle counter, which together measure, as an SMPS sys-

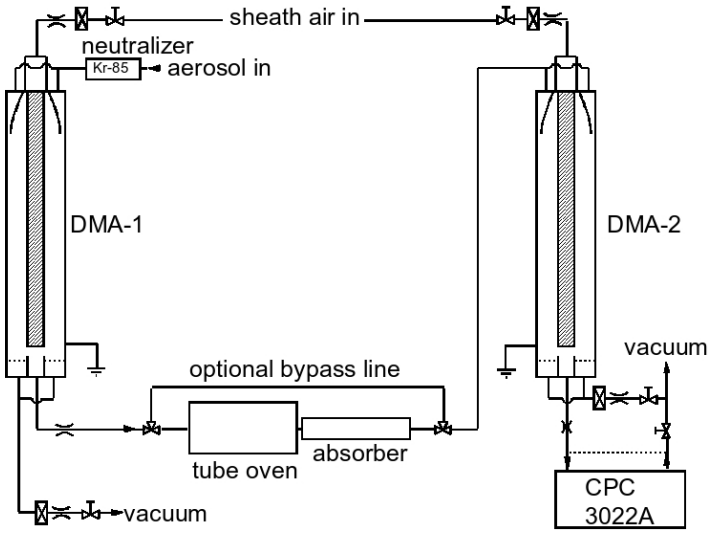

Figure 3.1. Schematic illustration of the volatility tandem differential mobility analyzer (VTDMA) system.

tem, the resulting particle size distribution after the conditioning process. As examples of conditioning devices, a humidifier has been used in particle hygroscopicity studies [*McMurry and Stolzenburg*, 1989], a reaction chamber in reactivity studies [*McMurry et al.*, 1983], and a thermodenuder (a heating unit and an absorbing unit) in particle volatility studies [*Rader et al.*, 1987; *Rader and McMurry*, 1986].

In this thesis, a TDMA system with a thermodenuder (a tube oven and an absorber) (Figure 3.1; Figure 2 in Paper I), was used to estimate the volatile fraction at different stages of particle aging in the environmental chamber for particles emitted from wood combustion [Paper I] and diesel engine [Paper II], and the volatile fraction of particles emitted from passenger cars [Paper V]. In this volatility TDMA (VTDMA) the quasi-monodisperse aerosol selected with the DMA-1 was heated in a temperature-controlled tube oven, cooled subsequently in a 50 cm long water-cooled (approximately at 10 °C) active charcoal absorber, and the resulting aerosol was measured with an SMPS system consisting of the DMA-2 and CPC. The active charcoal absorber was used in order to minimize re-condensation of the evaporated compounds on the particles, although thermodenuders without an absorber also can be used with a good removal efficiency [*Sakurai et al.*, 2003; *Orsini et al.*, 1999].

The heating zone of the oven was 40 cm long and the aerosol was flowing in a 2.2 cm i.d. stainless steel tube with a volumetric flow rate of 0.6–1.8 l/min (liters per minute). With these settings the average residence time in the heating zone was 5–15 s. In the 50 cm long cooler/absorber the aerosol was flowing in a 1.2 cm i.d. metal grid tube surrounded by the active charcoal (granular 3–5 mm) absorbent. The residence time in the absorber section was 1.9–5.7 s.

In the outdoor chamber experiments [Paper I, Paper II] the VTDMA analysis was performed at two or three stages of the aerosol aging process: (1) in the beginning for fresh aerosol, (2) at one intermediate point for 8 or 16 hours aged aerosol and (3) in the end for approximately 24 hours aged aerosol. The third stage was first checked and the VTDMA analysis was carried out, if enough particles were left in the chamber. At each stage, the volatile fraction of the particles was analyzed at four temperatures: 20 °C (base case), 140 °C, 250 °C and 360 °C. These temperatures were chosen based on previous work [*Leskinen*, 1997] from a wider set of temperatures. At each temperature, 1–3 particle sizes between 50–200 nm were chosen, depending on the prevailing particle size distribution in the chamber. For each sample, 1–2 scans with the SMPS were performed. With these parameters, the total VTDMA analysis cycle at each stage lasted two hours at its longest. This may have caused fluctuation in the results if the combustion aerosol composition was changing during the analysis cycle. For better time resolution several parallel preheated lines at selected temperatures can be used [*Philippin et al.*, 2004].

In the passenger car exhaust experiments [Paper V] the VTDMA analysis was performed at different steady state driving conditions (engine speed and load) for the inspected vehicles and fuels. In these experiments the temperatures of the denuding unit were 20 °C (base case), 75 °C, 150 °C, 225 °C, and 300 °C.

By comparing the volatilities of particles obtained by the VTDMA method altered primary particles can be distinguished from secondary particles formed by nucleation. With the VTDMA method, as small changes as 0.3 % in particle size of sub-0.2 μm particles can be detected [*Rader and McMurry*, 1986]. In some cases, when the particle has a non-volatile irregular shaped core and volatile material on it, as may be the case for diesel exhaust agglomerates [*Sakurai et al.*, 2003], the VTDMA method has been reported to underestimate the volatile fraction, because the volatile material released from the interstitial spaces of the agglomerates can not be detected with the VTDMA analysis, since the electrical mobility is conserved but mass is decreased. The underestimation of the volatile fraction for accumulation mode particles with low volatility can be as large as 70-90 %. This underestimation has also been discussed when comparing the results of volatility analysis and organic carbon analysis of diesel passenger car exhaust in Paper V.

Occasionally, also the polydisperse sample was analyzed with the thermodenuder [Paper I, Paper II, Paper V]. This gives information on the volatility of the whole aerosol population at the same scan. The analysis is much faster than VTDMA analysis, but misses the information about the behavior of monodisperse particles. However, it is very useful in fast changing situations and when long sampling times are not possible.

3.1.1.3 Electrical low-pressure impactor (ELPI)

An electrical low-pressure impactor (ELPI) [*Keskinen et al.*, 1992] was used in order to measure the particle size distribution of the generated mineral dust in the outdoor

chamber [Paper IV]. An ELPI consists of a unipolar charger, a cascade impactor and a multichannel electrometer. The charger is first used to charge the sample into a known unipolar charge level. In the cascade impactor the charged particles are classified into 12 size fractions according to their inertia, and consequently according to their aerodynamic diameter. The stages of the cascade impactor are electrically insulated from each other and each stage is connected to an electrometer. In some ELPI constructions, a filter stage, also connected to an electrometer, is used after the cascade impactor in order to collect the particles that have escaped the last impactor stage. The measured currents from the electrometers are converted in real time into a particle size distribution by using the known response function of the charger and the efficiency curves, or the kernels, of the impactor stages.

In this thesis the sample was drawn into the ELPI with a volumetric flow of 30 l/min and the size (aerodynamic diameter) range of 0.03–6.6 μm was monitored [Paper IV].

3.1.2 Filter collection and off-line particle analyses

3.1.2.1 Filter sampling setup and gravimetric analysis

In the outdoor chamber and passenger car experiments [Paper I, Paper II, Paper V], submicron particle samples were collected with a system consisting of a preimpactor and subsequent parallel lines of Teflon-quartz and quartz-quartz filters in series (Figure 4 in *Ålander* [2006]). The preimpactor was used before the filters in order to prevent larger particles and e.g. re-entrained particle clusters from entering the filter system. In the present sampling system the preimpactor had a 50 % cut point of 1 μm, which was chosen in order to produce mass concentration data comparable with the submicron SMPS analysis. After the preimpactor, the sample flow was divided equally between the two parallel lines and through the 47 mm Teflon (Pall Zefluor Supported PTFE 1.0 μm or Gelman Zefluor P5PL047) and 47 mm quartz fiber (Pallflex 2500QA(T/R)-UP) filters held in stainless steel filter holders (Gelman 2220).

The applied parallel filter setup, introduced by *Turpin et al.* [1994], was employed in order to correct for known positive artifact emerging from gas phase carbon adsorption on the quartz fiber filter. The sampling was continued until an analyzable amount (approximately 100 μg) of particles was expected to be collected on the quartz fiber filter. The sampling time ranged from 30–60 min for high particle concentrations to 2–4 h for lower particle concentrations in the chamber experiments [Paper I, Paper II]. In passenger car exhaust sampling, the sampling time was on the order of a few minutes [Paper V].

Prior to sampling the quartz fiber filters were pretreated by "baking" them in a furnace at 900 °C for 3 h in order to remove contaminants from the filters. The baked filters were stored in acid-washed and baked glass Petri dishes, sealed with a laboratory tape (Parafilm). Before weighing the filters with a microbalance (Mettler Toledo MT5,

accuracy 1 μg), they were conditioned in a controlled room at 20$\pm$1 °C and 40$\pm$1 % RH for 24 h. After preweighing, the filters were stored again in sealed Petri dishes, and just before sampling they were inserted into the filter holders. In order to prevent filter ruptures when tightening the holders, thin Teflon rings were used on both sides of the filter. The inner diameter of the rings was 37 mm, which was thus the diameter of the actual collection area on the filter. After sampling, the filters were conditioned and weighed as described earlier, and stored in the Petri dishes in a freezer at –18 °C in order to reduce loss of volatile material on the filters before organic and elemental carbon analysis. In every step of the filter handling and weighing procedure the filters were handled carefully and touched only with isopropyl alcohol rinsed tweezers on the filter edge, outside the collection area.

For both pre and postweighing, air density corrections due to changes in weighing room temperature, humidity and pressure were carried out by using the equation [*Mettler*, 1999]

$$m = R\frac{1 - a/8000\mathrm{kg/m^3}}{1 - a/\rho}, \tag{3.1}$$

where m is the corrected mass, R is the balance display, ρ is the density of the weighing sample (800 kg/m^3 for both Teflon and quartz fiber filters), and a is the air density (kg/m^3), given by

$$a = \frac{0.348444p - (0.00252t - 0.020582)h}{273.15 + t}, \tag{3.2}$$

where p is the ambient pressure (mbar), and h and t are the relative humidity (%) and the temperature (°C) of the weighing room.

3.1.2.2 Organic/elemental carbon (OC/EC) analysis

In order to produce additional information on the volatility of the particles, selected quartz fiber filters were analyzed with a thermal-optical transmission or reflectance (TOT/TOR) analysis [Paper I, Paper II, Paper V]. The method is described in Paper V and is described here only briefly. An 11 mm diameter (0.95 cm^2) punch of each filter was heated in an oven up to 800 °C in non-oxidizing Helium (100 %) atmosphere (30–550 °C) and oxidizing Helium(98 %)-Oxygen(2 %) atmosphere (550–800 °C). The released carbon was oxidized in a catalyst oven to CO_2, which was subsequently reduced to methane, which in turn was quantified by a flame ionization detector (FID). By using a calibration procedure for each sample, the masses of organic and inorganic carbon fractions and subfractions were obtained.

3.1.3 Analysis of gaseous compounds and meteorological parameters

In the chamber experiments [Paper I, Paper II, Paper III], inorganic gaseous pollutant concentrations were measured in order to monitor the injection and transforma-

tion of the aerosol, as well as ozone formation in the chamber. The gaseous compounds were measured by a chemiluminescent NO-NO_x analyzer (Environnement s.a., Model AC30M), a UV-absorption ozone analyzer (Dasibi, Model 1008-RS) and a UV-fluorescence SO_2 analyzer (Environnement s.a., Model AF21M). All analyzers were operated in the 0–1 ppm range. The sample to the analyzers was drawn from the chamber through a 4 mm i.d. Teflon line, which was 5 m long in the outdoor chamber experiments [Paper I, Paper II] and 1 m long in the indoor chamber experiments [Paper III]. In the outdoor chamber experiments, the Teflon line was kept at a temperature of 40–50 °C with a self-adjusting heating tape in order to minimize adsorption losses in the long line. Furthermore, the sample was drawn through a single line and split to the analyzers nearby in order to achieve the maximum sample flow rate (3.9 l/min) in the Teflon line. In all experiments, a 0.45 μm pore size Teflon prefilter was used to prevent particle transportation into the sample line and the analyzers.

In the outdoor chamber experiments [Paper I, Paper II], the total ultraviolet radiation (TUVR) and total solar radiation (TSR) in the chamber were measured with an Eppley Model TUVR radiometer (wavelengths 295–385 nm) and an Eppley Model PSP precision spectral pyranometer (wavelengths 295–2800 nm), respectively. The chamber air temperature and relative humidity were monitored with a Vaisala HMP233 meter in all chamber experiments [Paper I, Paper II, Paper III].

3.2 Examined aerosols

3.2.1 Wood combustion aerosol

Wood chips were combusted with a stoker burner attached to a domestic heating boiler of 20–40 kW nominal heat power output [Paper I]. The wood chips were spruce stem, 10–20 mm in size and irregular in shape. The water content of the combusted wood chips was determined from the mass decrease of a sample pile of the chips (gross weight 100–200 grams) when heated in an oven at 110 °C until the mass remained unchanged. The water content of the chips was approximately 20 % by mass.

In the stoker burner the chips are rationed from a container and transported by a revolving screw to the burner grate. Primary combustion air is premixed with the fuel in the transport screw. The screw rotation rate and combustion air flow rate can be adjusted manually to achieve constant combustion. Secondary combustion air can also be added to the flame zone through the secondary air hatch of the boiler.

The combustion was allowed to stabilize for 0.5–1 hours before injecting the aerosol into the chamber. During the stabilization period the combustion was monitored with a flue gas analyzer (Panametrics Model 300 Series) which measures the concentration of oxygen and combustible compounds (CO+H_2) in the flue gas. The target excess oxygen concentration was 13 %. When the combustion had stabilized, the combustion aerosol was transported to the chamber injection port through flue gas lines, which were insulated with glass wool coating, but not heated. The flue gas tem-

perature at the input to the chamber was approximately 40 °C. The flue gas residence time in the lines in this combustion setup was approximately 10 s.

3.2.2 Diesel engine exhaust

Diesel engine exhaust aerosol for aging studies [Paper II] was produced by a jeep (Toyota Land Cruiser), running at neutral gear at 1500 RPM. No specific attention was paid to the diesel fuel, but it was a mixture of commercial summer grade diesel fuels. The exhaust aerosol was transported to the chamber through the same flue gas lines as the wood chip combustion aerosol. The flue gas at the injection point was apparently at ambient temperature. In some experiments a diesel power aggregate (Perkins 103-10, nominal output power 12 kW) was operated below the environmental chamber. Neither in these experiments the fuel (commercial light fuel oil) was inspected in greater detail. In this setup due to shorter transfer line the residence time was 1–2 seconds and temperature at the input to the chamber around 100 °C.

For studies on the effects of fuel reformulation, exhaust after-treatment and engine operation on diesel engine exhaust particle volatility [Paper V], two diesel-powered passenger cars of different ages and engine types, using different types of fuels, were run on a chassis dynamometer. The exhaust was diluted in a dilution tunnel, equipped with a constant-volume sampler. The sample to the analyzers, such as the SMPS and VTDMA, was taken from the dilution tunnel. The sampling is described in more details in Paper V.

3.2.3 Mineral and metal dust

In the experiments described in Paper IV, mineral and metal dusts were generated by using a self-developed method exploiting an ejector, where pressurized air was pushed through a nozzle into the "throat" of a mixing chamber, causing an underpressure to the mixing chamber and suction from a dust container to the mixing chamber. A schematic picture of the dust generation system is given in Figure 2 in Paper IV.

The dust was injected into the chamber periodically, in order to maintain a predefined average dust concentration in the chamber. The concentration was monitored in real time with the ELPI described in 3.1.1.3. The concentration of inhalable dust varied between 0.8–8.7 mg/m^3 for mineral dust (quartz) and between 7.8–13.6 mg/m^3 for metal dust [Paper IV], with variations of $\pm$16–23 % in the concentration levels. The produced aerosol was monodisperse, with a calculated volume mean diameter of 2.9–3.0 μm for quartz dust and 3.4–3.6 μm for metal dust. For both dusts the calculated geometric standard deviation was 1.5.

3.3 ENVIRONMENTAL CHAMBERS

3.3.1 General

In as early as 1960s, smog chambers were used to demonstrate that certain atmospheric processes, such as ozone formation, occur [*Altshuller and Bufalini*, 1971]. The name "smog chamber" refers to studies of the processes which lead to photochemical smog formation. Later, these smog chambers with controllable conditions have been used to investigate e.g. the chemical and photochemical reactions of various mixtures of hydrocarbons and oxides of nitrogen in order to obtain experimental data for verification of chemical and photochemical models [e.g. *Finlayson-Pitts and Pitts*, 2000, pp. 871-886.]. In the first experiments only gaseous reactants and reaction products were under inspection. During the last decades also studies on particle formation and dynamics in the chambers have become popular.

Smog chambers are typically indoors, around 10 m^3 of volume, and equipped with UV lights, e.g. black light (350 nm) for photochemical reaction studies. The light intensity can be (apparently) constant over time or it can be varied, simulating natural diurnal sunlight changes. The results obtained in the smog chamber indoors with black light irradiation have been observed to be comparable to those observed outdoors with actual solar irradiation [*Laity*, 1971]. However, the results obtained in indoor smog chambers cannot be directly extrapolated to e.g. an urban atmosphere without caution.

Larger environmental chambers have also been constructed outdoors into natural conditions of light, temperature and humidity. In these chambers the conditions in the troposphere can be better simulated, minimizing the influence of meteorological phenomena and insertion of unwanted pollutants, which is an advantage compared to e.g. direct atmospheric measurements by aircraft or balloon [*Hughes et al.*, 2000].

The chamber walls may be fixed or the chamber may be collapsible. In a collapsible chamber, the sample air for analyzers need not be replaced, and the concentrations in the chamber are not changed subject to sampling. However, the experiment time is limited due to a limited volume of sample air. Collapsible bags can also be easily divided into "study" and "control" sections.

In fixed wall chambers, different air pressures can be applied in order to study the effect of pressure on the reactions, but the sample air has to be replaced e.g. with filtered air. This causes dilution of the compounds in the chamber and may lead to decreased reaction rates, at least in small chambers with a high sample flow rate.

The walls may also be permeable to gaseous compounds or gases, or particles may be adsorbed onto or desorbed from the walls. The walls may also act as a catalyst for some reactions. This is why the chamber material has to be as inert as possible. The most common material is polytetrafluoroethylene (PTFE), referred also as Teflon, which has been shown to suit well at least for high concentration experiments [*Kelly*, 1982]. Teflon is also available in very thin films which is important when considering light penetration, which depends on the light wavelength. For example, 95 % of the

350 nm UV light penetrates a 50 μm fluorinated ethylene-propylene copolymer (FEP Teflon) film, whereas e.g. Pyrex glass is known to absorb UV light in larger extent [*Finlayson-Pitts and Pitts*, 2000, p. 879], and is therefore not suitable for photochemical reactors. Of course, if for some reason, photochemical reactions are unimportant or unwanted, a non-transparent chamber material, such as stainless steel, is preferred.

An important chamber characteristic is the surface-to-volume ratio when estimating the chamber wall effects. In rigid wall chambers the surface-to-volume ratio is constant and the wall effects can be quite well estimated, but in collapsible chambers the surface-to-volume ratio increases with experiment time and this enhances the wall effects. In general, the lower the surface-to-volume ratio is, the lesser the wall effects are. However, it must be kept in mind that also other surfaces, such as suspended particulate matter, are usually available for heterogeneous reactions.

Wall effects, such as unknown heterogeneous reactions occurring on both fresh and conditioned chamber surfaces and release of uncharacterized reactive vapors from the previous experiments, are reported to be one of the largest uncertainties in chamber experiments [*Finlayson-Pitts and Pitts*, 2000]. Also deposition of particulate matter on chamber walls occurs, e.g. due to electrostatic effects [*McMurry and Rader*, 1985]. The wall materials, such as Teflon films, have been observed to emit contaminants [*Lonneman et al.*, 1981], such as carbon monoxide [*Kelly*, 1982]. Also ozone formation from "clean" air in new chambers has been observed [*Bufalini et al.*, 1977]. This is why new chambers are recommended to be "baked" by irradiating the chamber and leading simultaneously filtered air flow through the chamber for at least 24 hours. This should remove most hydrocarbon, NO_x and CO from the Teflon film. Also, in multiple experiments, the chamber material should be baked between the experiments, which was successfully employed e.g. by *Stern et al.* [1987].

3.3.2 Applied outdoor environmental chamber

The environmental (Figure 3.2) chamber at the University of Kuopio was constructed in 1997 in a research project focusing on aging studies of combustion aerosols. The chamber is mounted on a steel grating approximately 2 m above the university building rooftop. The space under the chamber serves as a place for measurement devices and a filtered air source, which consists of a powerful blower (1000 m^3/h) and EU4, EU9 and EU14 classified filters. The filtered air enters through a hatch in the chamber floor and the exhaust air exits through hatches in the chamber ceiling (see also Figure 1 in Paper I). The volume of the rigid wall chamber is 143 m^3 and the total surface area is 161 m^2, i.e. the surface-to-volume ratio is 1.1 m^{-1}. With the maximum filtered air flow rate the chamber air can thus be changed seven times in an hour. For aerosol injection, the chamber has a valve-controlled injection port equipped with a centrifugal blower (0.5 m^3/min).

The chamber walls and floor are made of 250 μm thick FEP Teflon film which

Figure 3.2. The outdoor environmental chamber at the Laboratory for Atmospheric Physics and Chemistry, University of Kuopio. The long walls of the chamber are in NW-SE orientation, NW end near the building behind the chamber. On the right is a wind shield.

is attached to stainless steel frames with aluminum profiles, using neoprene rubber seals in the seams. An aluminum foil is inserted under the floor film in order to enhance radiation in the chamber, to reduce radiative heating of the floor, and to even out temperature differences in the chamber. This is further enhanced by continuously mixing the chamber air with a fan, which has two 0.5 m wings and rotates at the rate of one revolution per second. The fan motor is located and operated outside the chamber to prevent motor carbon particle and axle lubricant oil emissions from entering the chamber. The exact temperature distribution in the chamber was not measured, but the chamber air was observed to reach a temperature of 40–50 °C on sunny days.

The chamber has been leak-tested by injecting a tracer gas, carbon dioxide (CO_2), to the chamber and by monitoring its concentration with an FTIR CO_2 analyzer at a measurement range of 0–3000 ppm. The initial CO_2 concentration was 2400 ppm and the relative tracer gas concentration decrease rate was approximately 0.025/h. After 60 hours the CO_2 concentration was 500 ppm and eventually reached the background level (390 ppm in this measurement). From this the overall chamber air dilution rate for CO_2 was estimated to be approximately 50 per cent in 24 hours. It must be noted

that the leak test was performed for one tracer gas only and may not be the same for other gases or particles. As direct measurement of particle leakage is difficult because of overlapping removal effects, such as wall losses and sampling, one has to estimate the leakage on the basis of a tracer gas leak test.

Altogether 23 experiments, 13 with wood chip combustion aerosol [Paper I] and 10 with diesel engine exhaust [Paper II], were conducted in the outdoor chamber. During combustion generated aerosol injection, the ceiling hatches were kept open, in order to keep ambient pressure in the chamber, and closed afterwards (Figure 1 in Paper I). The injection times varied from 1 to 7 min, which corresponds to 0.5–3.5 m^3 of flue gas, and an estimated dilution ratio from 1:300 to 1:40, respectively, when the flue gas mixed with the filtered air. The experiments started at various times of day and lasted 19–47 hours.

Prior to each experiment, the chamber was flushed for several hours with the particle filtered air and by exposing the chamber to sunlight, when available. This so called baking process intensified the desorption of earlier deposited material from the chamber walls. The desorbed material, as well as the suspended particles and vapors were removed from the chamber air. Between the experiment sets with different fuels, the chamber walls were cleaned with a mild detergent and rinsed thereafter with water by using a power washer.

The outdoor chamber was also used in the laboratory tests for different sampling methods and devices for inhalable and respirable dust [Paper IV]. In these experiments, mineral dust was generated by using the method described in 3.2.3 and injected to the chamber.

3.3.3 Applied indoor smog chamber

The indoor smog chamber (Figure 3.3) at the University of Kuopio is a 6 m^3 collapsible bag made of 50 μm thick FEP Teflon film. The bag is attached to stainless steel supporting frames and surrounded by two arrays of 34 pieces of 40-Watt Sylvania Blacklight 350 lamps on the opposite sides of the chamber. The produced 356 nm UV light penetrates the 50 μm FEP-teflon film almost completely (penetration 93 %). The lamps can be switched on all at the same time, giving total UV irradiance of 48 W/m^2, or in steps of 8 W/m^2. The chamber is also equipped with a fan with approximately 0.2 m wings in order to equalize the concentrations in the chamber volume.

Altogether nine experiments with xylene (a mixture of o-, m- and p-xylenes) and NO_x were conducted in the indoor smog chamber [Paper III]. Between the experiments, the chamber was flushed with dry, filtered air (temperature 20 °C, relative humidity 3 %) through injection and sampling ports. The filtered air was not completely free of NO_x, but the initial background NO_x level, mainly of nitrogen monoxide, was typically below 0.020 ppm.

Figure 3.3. The indoor smog chamber at the Laboratory for Atmospheric Physics and Chemistry, University of Kuopio.

3.4 COMPUTATIONAL METHODS

3.4.1 Growth rate calculations

The (total) growth rate for an aging aerosol in the environmental chambers [Paper I, Paper II, Paper IV] was calculated as the change rate of the geometric mean diameter d_{g} during a time period of Δt, i.e.

$$\mathrm{GR}_{\mathrm{total}} = \frac{\Delta d_{\mathrm{g}}}{\Delta t}. \tag{3.3}$$

The geometric mean diameter in Equation (3.3) was calculated by using Equation (2.2) and summing over all the measured size channels. The growth rate calculation was carried out in the beginning of each experiment and for the following night (in outdoor chamber experiments) and for the time when the condensation sink was approximately constant (in indoor chamber experiments). The Equation (3.3) was applied only when the particle size distribution was unimodal.

The growth arising from coagulation of particles in Paper I and Paper II was calculated by using Equation (2.4). The coagulation rate was approximated as self-coagulation for monodisperse aerosol with geometric mean diameter d_{g} (nm) and number concentration N (cm^{-3}).

3.4.2 Condensation sink calculations

For the indoor chamber experiments [Paper III] the concept of condensation sink [*Kulmala et al.*, 2001, 1998] was applied in order to estimate condensable vapor concentration C (cm^{-3}) and its source rate Q (cm^{-3}s^{-1}) as a function of time. These parameters were calculated from the size distribution data with geometric mean diameter of d_{g} (nm) and number concentration of N (cm^{-3}), giving the condensation sink [*Kulmala et al.*, 2001], and from the changes in the size distribution, giving the particle growth rate (Equation 3.3). In the calculation of the source rate, the vapor concentration was assumed constant and the source rate was approximated as the product of vapor concentration and condensation sink.

Calculating the vapor concentration and its source rate gives valuable additional information on the formation and growth properties of nucleation mode aerosol particles. They can also be applied in estimation of the basic composition properties of the newly formed particles. These quantities also serve as a measure when aerosol formation and growth in different environments, such as a heavily polluted urban area and a very clean background area, are compared.

4 MAIN RESULTS

4.1 PARTICLE SIZE AND GROWTH DURING AGING

The particle size distributions of the freshly emitted combustion aerosols were observed to be unimodal, with a geometric mean diameter of 72–86 nm for the wood combustion aerosol [Paper I], 66–85 nm for the diesel-powered off-road engine exhaust [Paper II], 63–77 nm for the exhaust from the passenger car with an indirect injection engine [Paper V], and 102–115 nm for the exhaust from the passenger car with a direct injection engine [Paper V]. The particle size was observed to depend on the operation parameters of the wood combustion device and the diesel engines. For example, in wood combustion, lower excess oxygen concentration in the flue gas (9 % vs. 13 %), i.e. less oxygen in combustion, was observed to produce larger particles [Paper I], which is similar to the observations of *Hueglin et al.* [1997]. The size of the particles from the passenger car was found to depend on the engine speed, power output, type, and fuel. For example, the passenger car equipped with a direct injection engine produced approximately 30–40 nm larger particles than the passenger car equipped with an indirect injection engine [Paper V]. However, this finding differed from the findings of e.g. *Maricq et al.* [2002] who observed significantly lower particle sizes from a light-duty direct injection diesel engine. As discussed in Paper V, it was suggested that this discrepancy may have emerged from the characteristics of the individual engine.

In the aging experiments of both wood combustion aerosol and diesel engine exhaust, the particles were observed to grow and their number concentration was observed to decrease after they had been released into the environmental chamber. The particle diameter growth rate was highest during the first hour, being 17–28 nm/h for the wood combustion aerosol particles and 18–47 nm/h for the diesel particles. Later on, the growth rate was observed to decrease, being lowest during the nights, less than 1 nm/h, on an average. In the indoor smog chamber experiments for verification of particle formation from gaseous precursors formed in the photooxidation of xylene and NO_x, the particles were observed to subsequently grow to around 100 nm size at a growth rate of 8–26 nm/h. The growth rates observed in the chambers exceed those observed in the atmosphere, and are even higher than those observed in a heavily polluted area of New Delhi [*Kulmala et al.*, 2005]. In order to sustain the growth rates observed in the chamber experiments, condensable vapor concentrations of $1.1\text{–}3.6\times10^8$ cm^{-3} are required, corresponding to vapor source rates of $0.15\text{–}4.4\times10^7$ cm^{-3}s^{-1} [Paper III]. The calculated source rates of condensable vapors in the chamber are several orders of magnitude higher than those observed in the atmosphere in the background stations and correspond those in a heavily polluted area, as observed by *Kulmala et al.* [2005].

The main processes leading to the above mentioned growth of particles are coagulation and condensation. For example, of the growth rates observed in the environmental chamber, the contribution of coagulation to the particle growth was estimated to be approximately 50 % in the wood combustion aerosol experiments [Paper I] but only

12–35 % in the diesel engine exhaust experiments [Paper II]. These calculated results together with the observations that the initial particle size and number concentration for both aerosols were of the same magnitude (72–86 nm and 2.1–3.7$\times 10^5$ cm^{-3} for wood combustion aerosol [Paper I], and 66–85 nm and 0.9–4.6$\times 10^5$ cm^{-3} for diesel engine exhaust [Paper II], respectively) suggest that there were more condensable vapors in the diesel engine exhaust particles than in the wood combustion aerosol particles. Also polymerization of organic compounds in the particles may have occurred, leading to the growth of the less volatile core of the particles, similar to that observed for atmospheric particles by *Ehn et al.* [2007] and *Wehner et al.* [2005].

4.2 Particle volatility and its change during aging

The volatility of fresh wood combustion aerosol particles was found to increase with the oven temperature, i.e. the higher the temperature, the larger the size decrease at that temperature. The volatility of fresh particles was found quite low, as only 20–32 % of volume (6–10 % of diameter) evaporated at 360 °C. The low volatility of fine particles from a similar kind of wood chip burner was also observed by *Hueglin et al.* [1997]. Furthermore, the degree of volatility was found to depend on the time of day when the experiment started. The volatility of the fresh particles was highest in the experiments that started in the afternoon and lowest in the experiments that started in the evening. For example, the decrease in diameter of the fresh 200 nm particles was 20 nm in the experiments that started in the afternoon, but 8–11 nm in the experiments that started in the evening [Paper I].

The volatility of the wood combustion aerosol particles was also observed to increase with aging to 14–71 % (10–68 % for diameter) for 8–12 h aged aerosol, and to 98–99 % (74–86 % for diameter) for 24 h aged aerosol [Paper I]. Possible pathways leading to the higher volatility are discussed in Figure 6 in Paper I and include e.g. change in particle composition by condensation of more volatile compounds on the particles or photodegradation of less volatile compounds into more volatile compounds.

A similar kind of increase in the volatility of the diesel engine exhaust particles with aging was observed, when the diesel engine was run without load [Paper II]. The volatile volume fraction of the freshly emitted particles was 37–45 % and that of 8 h aged particles 56–63 % at 360 °C. When the diesel engine was run with a 9 kW (75 %) load, the fresh exhaust particles contained less volatile material, as only 10–24 % of the apparent volume was found volatile at 140 °C and even a smaller fraction, 10–19 % of volume, at 360 °C (Figure 3b in Paper II). The volatile fraction decreased further with particle aging, being 7 % of volume at 140 °C and 14 % of volume at 360 °C after 18 h of aging. This indicates that the fresh particles contained some volatile material that evaporated into the chamber during the experiment.

Also the volatility of the particles from the jeep engine was found to increase when the particles aged. The volatile fraction on the freshly produced particles was found to

be 22–57 % at 360 °C, and on 24 h aged particles 78 % at 140 °C and 99 % at 360 °C (Figure 3c in Paper II).

The volatile volume fraction of the freshly emitted particles was found to depend on the engine load. By increasing the engine load from 0 kW to 9 kW, the volatile fraction decreased from 37–45 % to 10–19 % at 360 °C [Paper II]. This is similar to the observations by *Philippin et al.* [2004] and *Kwon et al.* [2003], who found that an increasing engine load decreased the amount of volatile material on the particles emitted by medium-duty diesel-fueled vehicles. A similar observation was made for the jeep engine exhaust particles. For example, 50 % of the volume of fresh 50 nm particles produced by the idling jeep engine was found volatile at 250 °C, which is significantly more than the 2–25 % observed by *Philippin et al.* [2004] with higher engine speeds.

For diesel passenger cars with higher load (3.5–20 kW) the change in particle diameter due to heating was much lower than for the jeep engine exhaust in the chamber experiments. The maximum change in particle diameter was 7 nm in 150 nm particles [Paper V], although higher volatility of diesel engine exhaust particles have been observed in similar experiments by *Kwon et al.* [2003].

In the fresh diesel engine exhaust particles, the volatile fraction was found to evaporate already at the lowest oven temperature (140 °C). With aging, the particles were transformed into less volatile, which was observed as smaller volatile fraction at 140 °C but larger volatile fraction at 250 °C and at 360 °C than in the fresh particles at the same temperatures (Figures 3a and 3b in Paper II). This suggests that during aging less volatile compounds had been condensed on the particles, or that the lower volatility was due to intra-particle oligomerization, as discussed in Paper II.

4.3 Particle carbon content and its change during aging

In this work, the mass fraction of organic carbon in the fresh wood combustion particles was observed to be very low, 4.8 %. This is substantially less than the organic mass fractions in biomass combustion aerosols observed by *Iinuma et al.* [e.g. 2007]. They found that in the aerosol from the combustion of spruce with green needles the bulk fine particle mass emission factor was 5800 mg/kg and of that 2120 mg/kg, i.e. 37 % of mass was organic carbon. The observed low organic mass fraction in this work is likely due to the quite efficient burning of the wood chips. The organic mass fraction was, however, observed to increase with aging to 17 % for 8 h aged and 24 % for 24 h aged particles [Paper I]. At the same time, the particulate organic to total carbon fraction increased from 63 % (fresh) to 68 % (8 h aged) and to 79 % (24 h aged) and the fraction of more volatile organic carbon (OC2 to total OC ratio) increased from 25 % to 33 % and that of less volatile organic carbon (OC4 to total OC ratio) decreased from 16 % to 13 % (Figure 4 in Paper I). One possible explanation for this is degradation of less volatile compounds into more volatile ones, like the PAH photodegradation observed

by *Kamens et al.* [1988]. The increasing OC fraction in the particles as they age agrees qualitatively with the VTDMA analysis results.

The mass fraction of organic carbon in the fresh diesel particles was 13.1 % when the engine was run without load and 7.1 % when the engine was run with 9 kW load. The organic emissions are low but consistent with observations of e.g. *Kittelson* [1998]. The organic mass fraction, as well as the organic to total carbon fraction in the particles from the diesel engine without load was observed to increase with aging. The organic to total carbon fraction increased from 72 % to 91 % during a 8 h aging period, which is consistent qualitatively with the VTDMA analysis results. In the exhaust particles emitted by the diesel engine with 9 kW load, the organic to the total carbon fraction was observed to decrease from 58 % to 39 % (Figure 4b in Paper II). This is in agreement with the VTDMA analysis performed for the same aerosol (Figure 3b in Paper II) and suggests that the fresh particles contained species which evaporated into the chamber during the 18 h aging period.

4.4 New particle formation and growth

In the outdoor chamber experiments, new particle formation was observed, usually in the following morning, when the surface area of the pre-existing aerosol particles had decreased low enough and when enough sunlight was available [Paper I, Paper II]. In the indoor chamber experiments without these so called seed particles, the new particles were observed to form rapidly after the UV lights had been turned on [Paper III]. In the indoor chamber the new particle formation is linked to the photooxidation of xylene. The oxidants were formed by the photochemical reactions of NO_2 dissociation and subsequent oxygen radical and ozone formation. An ozone concentration of 0.010–0.038 ppm was observed in wood combustion aerosol experiments, when the NO concentration in the chamber had sunk low enough [Paper I], but in the diesel engine exhaust experiments, no ozone formation was observed regardless of lowered NO concentration [Paper II]. On the contrary, in the indoor chamber experiments, ozone formation was found intensive, and as high ozone concentrations as 0.79 ppm were observed [Paper III].

When the new particle formation in the smog chamber experiments, by using an estimated time when the particles were 3 nm in diameter, was coupled to the injected HC/NO_x ratio it was found that, in the inspected range of 3.5 to 30, the particle formation is fastest with the HC/NO_x ratio of approximately 10–20. With lower HC/NO_x ratios, the particle formation was estimated to have started 5–24 min later. Also, when comparing the source rate with the initial HC/NO_x ratio, it was found highest for the HC/NO_x ratio of 8. The initial NO_x concentration was observed to influence the source rate, but the initial hydrocarbon concentration not.

4.5 Errors and uncertainties in the measurements and analyses

The uncertainties in the on-line measurements arise from e.g. particle losses in the sampling lines and particle instruments, as well as from the geometry and detection capabilities of the instruments. In the off-line analyses the uncertainties arise from e.g. losses of volatile material from the filters before the analysis.

The proposed mechanisms for the particle losses during the sample transport through sampling lines and instruments are gravitational settling, diffusional deposition, inertial deposition at bends, flow constrictions and turbulent regions, and electrostatic, thermophoretic and diffusiophoretic deposition [e.g. *Baron and Willeke*, 2001]. In practise, for submicron particles studied in this thesis, the diffusional deposition losses are the most important while the others can be neglected, apart from the thermophoretic losses in the thermodenuder arising from differences in the temperatures of the tube wall and gas. Especially, in the beginning of the cooling section, where the wall temperature suddenly drops below that of the gas, the thermophoretic losses may be increased.

The diffusional deposition in the sampling tubes depend e.g. on the tube diameter and the flow rate in the tube. In the experiments in this thesis, a 4 mm (inner diameter) tube was usually used for sample transport. The penetration through 1 m of this tube was estimated to be 42 %, 91 % and 99 % for 3 nm, 15 nm and 200 nm particles, respectively. The DMA types used in this thesis are reported to have a 51–99 % penetration for 2–66 nm particles and a 89–99 % penetration for 15–750 nm particles [*Pyykönen et al.*, 2007]. The total penetration of the initially 50–200 nm sized particles through the thermodenuder was estimated to be 97–99 % with the tube oven temperature of 360 °C. It must be noted that the penetration may be remarkably lower when the size of the particles has decreased due to particle evaporation in the heating section of the thermodenuder. For example, the penetration through the thermodenuder is 88 % for a 15 nm particle, and only 34 % for a 3 nm particle.

Some errors may also arise from the fact that the selected particles by the DMA are not all of the same size, as described in 3.1.1.1. For example, approximately 20 % of the "100 nm sized" particles at the DMA outlet are doubly charged, when a uniform particle size distribution at the DMA inlet is assumed. In practise, the fraction of the multiply charged particles may be even larger, depending on the particle size distribution at the DMA inlet and the selected particle size. In this thesis, the multiple charge correction of the SMPS measurement software was used in order to minimize this effect. The aerosol at the DMA outlet also contains particles of different sizes due to diffusion in the DMA [e.g. *Alonso and Kousaka*, 1996]. This effect is strongest for nanoparticles and can be neglected for the particle sizes used in the VTDMA analysis in this thesis.

The condensation particle counters have been reported to suffer from coincidence phenomenon, as described in 3.1.1.1. For example, in the CPC model used in this thesis, the effect of coincidence becomes important at particle concentrations above 10^4 cm^{-3}. However, in the SMPS and VTDMA analyses, the concentrations registered by the CPC

were well below this concentration level and therefore the effect of coincidence can be neglegted. Also the counting efficiency of the used CPC was unity for the analyzed size regions.

When the filters were prepared for the gravimetric and carbon analyses, some loss of volatile material from the filters may have occurred, especially during the 24 h conditioning period. This may have been the reason for very low masses of the observed OC1 fraction, for which the evaporation losses are considered highest.

5 REVIEW OF THE PAPERS

This thesis consists of five original papers. The major contributions of the individual papers are as follows.

In Paper I the aging of emission from wood chip combustion in a stoker burner was monitored in a 143 m^3 outdoor environmental chamber (described in 3.3.2) for 19–27 h in order to study the size distribution, volatility and organic carbon content of the combustion aerosol particles during aging. The analysis was based on the on-line measurements of the particle size distribution with a scanning mobility particle sizer (SMPS) system (described in 3.1.1.1) and the size evolution of different sized monodisperse particles with a volatility tandem differential mobility analyzer (VTDMA) system (described in 3.1.1.2) and gaseous compound measurements, as well as the off-line gravimetric and thermal-optical carbon analyses of collected samples on Teflon and quartz fiber filters, respectively. The VTDMA analysis was performed in the beginning, after 8–12 h of aging, and after 24 h of aging. The carbon analysis was performed for the filter samples collected during the VTDMA analyses. The VTDMA and carbon analysis results were compared with each other qualitatively.

Paper II describes overnight aging experiments in the environmental chamber described in 3.3.2 with diesel engine exhaust from a diesel power aggregate, by applying no or 9 kW load, and from a diesel-fueled vehicle. The volatilities of monodisperse particles of several sizes were analyzed with VTDMA analysis described in 3.1.1.2. The particulate organic to total carbon ratio and organic carbon subfractions (volatile at 120 °C, 250 °C, 450 °C and 550 °C) were analyzed with thermal-optical carbon analysis (section 3.1.2.2) for samples from fresh, 8 or 18 h aged and 24 h aged aerosol. During the experiment also the particle size distribution, ozone and nitrogen oxide concentrations, temperature, relative humidity and total solar and total ultraviolet radiation in the chamber were monitored.

In Paper III the formation and subsequent growth of pure organic aerosol particles were investigated in laboratory conditions. A mixture of an aromatic hydrocarbon (HC) and nitrogen oxides (NO_x) was irradiated with 350 nm UV light in a 6 m^3 teflon chamber (described in 3.3.3). Various mixtures with HC/NO_x ratios from 3.5 to 30 were applied. The changes in particle size distribution were monitored in the range of 7–330 nm for 150–180 min with an SMPS system. The concept of condensation sink was applied to the measured size distribution data in order to estimate the concentration and source rate of condensable vapor in the chamber with the method described in 3.4.2.

In Paper IV the performances of four sampling devices for inhalable dust and three devices for respirable dust were investigated both in the laboratory and in the field. The laboratory experiments were conducted in the outdoor environmental chamber. Mineral and metal dusts were generated into the chamber by using a self-developed dust blower. The introduced particle size distribution in the chamber was monitored

continuously by using an electrical low-pressure impactor (described in 3.1.1.3) in the size range of 0.03–6.6 μm. In the field measurements, which were carried out in a talc production plant, a metal smelter, a metal foundry, and a peat-fired power plant, also peat dust was examined. An IOM (Institute of Occupational Medicine) sampler was chosen as the reference method for inhalable dust, and the IOM sampler provided with the porous plastic foam media was used as the reference method for respirable dust. The other instruments tested were a Button sampler, an optical Grimm aerosol monitor, and a Dekati two-stage cascade impactor with cut-off sizes of 10 and 4 μm. The main emphasis of the study was on the respirable sampling of the instruments.

In Paper V the effects of fuel reformulation, oxidation catalyst, engine type, and engine operation parameters on diesel particle emission characteristics, such as particle size distribution (SMPS), organic and elemental carbon fractions (thermal-optical carbon analysis), and the particle volatility (VTDMA), were investigated. The experiments were carried out with two diesel-powered passenger cars, the other equipped with an oxidation catalyst and an exhaust gas recirculation system, on a chassis dynamometer in an engine laboratory.

6 CONCLUSIONS

This thesis presents studies on different kinds of aerosols, and their formation and aging. The main findings of this work are as follows.

The particle size and number concentrations were typical for combustion aerosols after dilution, and in all experiments the particle size distribution was unimodal. As the particles aged, their size increased and concentration decreased [Paper I, Paper II, Paper III]. The size increase arises from two typical processes in particle dynamics: condensation and coagulation. The latter also decreases the number concentration. From the calculated fractions of the particle growth by coagulation for aerosols from different sources, it was concluded that in diesel engine exhaust there were more condensable vapors in the chamber than in wood combustion aerosol. This may well have been the case, as the diesel engine exhaust was injected to the chamber at higher temperature and through a shorter transfer line with less losses of condensable vapors to the transfer line than with the wood combustion aerosol. It is therefore suggested that a transfer line as short as possible is to be used in order to maintain the aerosol as unchanged as possible until the actual measurements.

The volatility of the freshly emitted particles was found to change with the source and with aging. The increased volatility due to aging can be explained with the growth of particles by condensation, which increases the volatile fraction on the particles, or it may have increased e.g. in photodegradation of the less volatile organic compounds on the particles into more volatile compounds. The different possible pathways to increased volatility have been discussed in more detail in Paper I.

The overall volatility of the particle population increased also when new particles were formed. These new particles were high in number and they were found almost completely volatile [Paper I, Paper II]. From this it can be concluded that new particle formation plays an important role when volatility of an atmospheric particle population is concerned. New particle formation was also observed in controlled conditions as a result of photooxidation of known pollutants in urban environments, xylene and nitrogen oxides [Paper III]. All these newly formed particles were observed to grow subsequently to approximately 100 nm size.

The calculated vapor source rates were observed to depend on the initial concentrations of organic compound and nitrogen oxides, as well as the ratio of their concentrations. The source rate was observed to be highest and the particle formation was observed to occur fastest at the same initial HC/NO_x ratio. As the source rate was found to be proportional of the initial NO_x concentration it was concluded that oxidation processes play an important role in particle formation.

The answers to the questions presented in Chapter 1 are threefold and as follows:

1. *Is the volatility tandem differential analysis (VTDMA) a relevant on-line method for estimating the organic fraction of aerosol particles, at least qualitatively?*

   Yes. In the chamber experiments with wood combustion aerosol [Paper I] and

diesel engine exhaust [Paper II] a qualitative agreement between the on-line VTDMA method and the off-line carbon analysis was found. In Paper V also a good quantitative agreement was observed between these two analysis methods. These observations indicate that the VTDMA analysis is well applicable also for estimation of the organic carbon fraction.

Suggestions for further work:

The method should be developed for better time resolution. For example, in this work, the completion of the selected measurement set for the VTDMA analysis lasted two hours. This is not a problem when performing the analysis for a steady process, such as the passenger car exhaust by using a chassis dynamometer, but for non-steady processes, such as aerosol aging, an improved analysis should be used.

2. *Do the aging of wood combustion aerosol and diesel engine exhaust differ from each other?*

   Even if the aerosol from these two sources were almost similar according to their size distribution and carbon content, differences in their aging were observed. The contribution of coagulation on the growth rate was found to be higher for wood combustion particles than for diesel engine exhaust particles, indicating greater contribution of growth of diesel particles by condensation.

3. *How do the aerosol processes in environmental chambers compare to the processes in the atmosphere?*

   They might be overestimated. In the outdoor chamber the irradiation was, of course, the same magnitude as in the atmosphere, but in the indoor chamber with UV lamps the UV irradiation was stronger than usually in the atmosphere. This results in increased reaction rates. Also the particle concentrations were higher than atmospheric concentrations but rather represented the concentrations near a stack or exhaust pipe, or those in a heavily polluted area.

   Suggestions for further work:

   More experiments with concentrations comparable to atmospheric concentrations should be carried out. The chambers could also be divided into two halves in order to enable simultaneous measurements of e.g. aerosols from different sources or different reactants (including clean air), or same aerosols or reactants but with different initial concentrations. This is important at least for experiments in the outdoor chamber, as the prevailing conditions cannot be accurately reproduced.

REFERENCES

Ålander, T., Carbon composition and volatility characteristics of the aerosol particles formed in internal combustion engines, Ph.D. thesis, University of Kuopio, Finland, 2006.

Alonso, M., and Y. Kousaka, Mobility shift in the differential mobility analyzer due to Brownian diffusion and space-charge effects, *J. Aerosol Sci.*, *27*, 1201–1225, 1996.

Altshuller, A., and J. Bufalini, Photochemical aspects of air pollution. A review, *Environ. Sci. Technol.*, *5*, 39–64, doi:10.1021/es60048a001, 1971.

Baron, P., and K. Willeke, *Aerosol measurement: Principles, techniques, and applications*, John Wiley and Sons, 2001.

Bufalini, J., T. Walter, and M. Bufalini, Contamination effects on ozone formation in smog chambers, *Environ. Sci. Technol.*, *11*, 1181–1185, 1977.

Dentener, F., G. Carmichael, Y. Zhang, J. Lelieveld, and P. Crutzen, Role of mineral aerosol as a reactive surface in the global troposphere, *J. Geophys. Res.*, *101*, 22,869–22,889, 1996.

Ehn, M., T. Petäjä, W. Birmili, H. Junninen, P. Aalto, and M. Kulmala, Non-volatile residuals of newly formed atmospheric particles in the Boreal forest, *Atmos. Chem. Phys.*, *7*, 677–684, 2007.

Finlayson-Pitts, B., and J. Pitts, *Chemistry of the upper and lower atmosphere*, Academic Press, 2000.

Fuzzi, S., et al., Critical assessment of the current state of scientific knowledge, terminology, and research needs concerning the role of organic aerosols in the atmosphere, climate, and global change, *Atmos. Chem. Phys.*, *6*, 2017–2038, 2006.

Girshick, S., and C.-P. Chiu, Kinetic nucleation theory: A new expression for tht rate of homogeneous nucleation from an ideal supersaturated vapor, *J. Chem. Phys.*, *93*, 1273–1277, 1990.

Haynes, B., and H. Wagner, Soot formation, *Prog. Energy Combust. Sci.*, *7*, 229–273, 1981.

Hering, S., M. Stolzenburg, F. Quant, D. Oberreit, and P. Keady, A laminar-flow, water-based condensation particle counter (WCPC), *Aerosol Sci. Technol.*, *39*, 659–672, 2005.

Hinds, W., *Aerosol technology. Properties, behavior, and measurement of airborne particles*, 2nd ed., John Wiley & Sons, Inc., New York, USA, 1998.

Holmes, N., A review of particle formation events and growth in the atmosphere in the various environments and discussion of mechanistic implications, *Atmos. Environ.*, *41*, 2183–2201, 2007.

Hueglin, C., C. Gaegauf, S. Künzel, and H. Burtscher, Characterization of wood combustion particles: morphology, mobility, and photoelectric activity, *Environ. Sci. Technol.*, *31*, 3439–3447, 1997.

Hughes, L., J. Allen, P. Bhave, M. Kleeman, G. Cass, D.-Y. Liu, D. Fergenson, B. Morrical, and K. Pragher, Evolution of atmospheric particles along trajectories crossing the Los Angeles basin, *Environ. Sci. Technol.*, *34*, 3058–3068, 2000.

Iinuma, Y., E. Brüggemann, T. Gnauk, K. Müller, M. Andreae, G. Helas, R. Parmar, and H. Herrmann, Source characterization of biomass burning particles: The combustion of selected European conifers, African hardwood, savanna grass and German and Indonesian peat, *J. Geophys. Res.*, *112*, 8209, 2007.

IPCC, Summary for policymakers, in *Climate Change 2007: The Physical Science Basis. Contribution of Working Group I to the Fourth Assessment Report of the Intergovernmental Panel on Climate Change*, edited by S. Solomon, D. Qin, M. Manning, Z. Chen, M. Marquis, K. Averyt, M. Tignor, and H. Miller, Cambridge University Press, Cambridge, United Kingdom and New York, NY, USA, 2007.

Jang, M., N. Czoschke, S. Lee, and R. Kamens, Heterogeneous atmospheric aerosol production by acid-catalyzed particle-phase reactions, *Science*, *298*, 814–817, 2002.

Kalberer, M., et al., Identification of polymer as major components of atmospheric organic aerosols, *Science*, *303*, 1659–1662, 2004.

Kamens, R., G. Rives, J. Perry, D. Bell, J. P. R.F, R. Goodman, and L. Claxton, Mutagenic changes in dilute wood smoke as it ages and reacts with ozone and nitrogen dioxide: An outdoor chamber study, *Environ. Sci. Technol.*, *18*, 523–530, 1984.

Kamens, R., Z. Guo, J. Fulcher, and D. Bell, Influence of humidity, sunlight, and temperature on the daytime decay of polyaromatic hydrocarbons on atmospheric soot particles, *Environ. Sci. Technol.*, *22*, 103–108, 1988.

Kelly, N., Characterization of fluorocarbon-film bags as smog chambers, *Environ. Sci. Technol.*, *16*, 763–770, 1982.

Keskinen, J., K. Pietarinen, and M. Lehtimäki, Electrical low pressure impactor, *J. Aerosol Sci.*, *23*, 353–360, 1992.

Kittelson, D., Engines and nanoparticles: A review, *J. Aerosol Sci.*, *29*, 575–588, 1998.

Knutson, E., and K. Whitby, Aerosol classification by electric mobility: Apparatus, theory and applications, *J. Aerosol Sci.*, *6*, 443–451, 1975.

Korhonen, P., M. Kulmala, A. Laaksonen, Y. Viisanen, R. McGraw, and J. Seinfeld, Ternary nucleation of H_2SO_4, NH_2, and H_2O in the atmosphere, *J. Geophys. Res.*, *104*, 26,349–26,353, 1999.

Kulmala, M., and A. Laaksonen, Binary nucleation of water–sulphuric acid system: Comparison of classical theories with different H_2SO_4 saturation vapor pressures, *J. Chem. Phys.*, *93*, 696–701, 1990.

Kulmala, M., A. Toivonen, J. Mäkelä, and A. Laaksonen, Analysis of the growth of nucleation mode particles observed in Boreal forest, *Tellus*, *50B*, 449–462, 1998.

Kulmala, M., M. D. Maso, J. Mäkelä, L. Pirjola, M. Väkevä, P. Aalto, P. Miikkulainen, K. Hämeri, and C. O'Dowd, On the formation, growth and composition of nucleation mode particles, *Tellus*, *53B*, 479–490, 2001.

Kulmala, M., H. Vehkamaki, T. Petaja, M. D. Maso, A. Lauri, V.-M. Kerminen, W. Birmili, and P. McMurry, Formation and growth rates of ultrafine atmospheric particles: A review of observations, *J. Aerosol Sci.*, *35*, 143–176, 2004.

Kulmala, M., T. Petäjä, P. Mönkkönen, I. Koponen, M. D. Maso, P. Aalto, K. Lehtinen, and V.-M. Kerminen, On the growth of nucleation mode particles: Source rates of condensable vapor in polluted and clean environments, *Atmos. Chem. Phys.*, *5*, 409–416, 2005.

Kulmala, M., K. Lehtinen, and A. Laaksonen, Cluster activation theory as an explanation of the linear dependence between formation rate of 3 nm particles and sulphuric acid concentration, *Atmos. Chem. Phys.*, *6*, 787–793, 2006.

Kulmala, M., et al., Toward direct measurement of atmospheric nucleation, *Science*, *318*, 89–92, 2007a.

Kulmala, M., et al., The condensation particle counter battery (CPCB): A new tool to investigate the activation properties of nanoparticles, *J. Aerosol Sci.*, *38*, 289–304, 2007b.

Kwon, S.-B., K. Lee, K. Saito, O. Shinozaki, and T. Seto, Size-dependent volatility of diesel nanoparticles: Chassis dynamometer experiments, *Environ. Sci. Technol.*, *37*, 1794–1802, 2003.

Laity, J., A smog chamber study comparing blacklight fluorescent lamps with natural sunlight, *Environ. Sci. Technol.*, *5*, 1218–1220, 1971.

Lee, S.-H., J. Reeves, J. Wilson, D. Hunton, A. Viggiano, T. Miller, J. Ballenthin, and L. Lait, Particle formation by ion nucleation in the upper troposphere and lower stratosphere, *Science*, *301*, 1886–1889, 2003.

Leskinen, A., Tandem DMA technique in structure analysis of combustion aerosol, Master's thesis, University of Kuopio, Kuopio, Finland, in Finnish, 1997.

Lonneman, W., J. Bufalini, R. Kuntz, and S. Meeks, Contamination from fluorocarbon films, *Environ. Sci. Technol.*, *15*, 99–103, 1981.

Maricq, M., R. Chase, N. Xu, and P. Laing, The effects of the catalytic converter and fuel sulfur level on motor vehicle particulate matter emissions: Light duty diesel vehicles, *Environ. Sci. Technol.*, *36*, 283–289, 2002.

McMurry, P., A review of atmospheric aerosol measurements, *Atmos. Environ.*, *34*, 1959–1999, 2000.

McMurry, P., and D. Rader, Aerosol wall losses in electrically charged chambers, *Aerosol Sci. Technol.*, *4*, 249–268, 1985.

McMurry, P., and M. Stolzenburg, On the sensitivity of particle size to relative humidity for Los Angeles aerosols, *Atmos. Environ.*, *23*, 497–507, 1989.

McMurry, P., H. Takano, and G. Anderson, Study of the ammonia (gas)–sulfuric acid (aerosol) reaction rate, *Environ. Sci. Technol.*, *17*, 347–352, 1983.

Mettler, *Weighing the Right Way with Mettler Toledo*, Mettler-Toledo GmbH, Switzerland, 1999.

Mordas, G., H. Manninen, T. Petäjä, P. Aalto, K. Hämeri, and M. Kulmala, On operation of the ultra-fine water-based CPC TSI 3786 and comparison with other TSI models (TSI 3776, TSI 3772, TSI 3025, TSI 3010, TSI 3007), *Aerosol Sci. Technol.*, *42*, 152–158, 2008.

Orsini, D., A. Wiedensohler, F. Stratmann, and D. Covert, A new volatility tandem differential mobility analyzer to measure the volatile sulfuric acid aerosol fraction, *Journal of Atmospheric and Oceanic Technology*, *16*, 760–772, 1999.

Philippin, S., A. Wiedensohler, and F. Stratmann, Measurements of non-volatile fractions of pollution aerosols with an eight-tube volatility tandem differential mobility analyzer (VTDMA-8), *J. Aerosol Sci.*, *35*, 185–203, 2004.

Pope, C., and D. Dockery, Health effects of fine particulate air pollution: Lines that connect, *Journal of Air and Waste Management Association*, *56*, 709–742, 2006.

Pyykönen, J., M. Miettinen, O. Sippula, A. Leskinen, T. Raunemaa, and J. Jokiniemi, Nucleation in a perforated tube diluter, *J. Aerosol Sci.*, *38*, 172–191, 2007.

Rader, D., and P. McMurry, Application of the tandem differential mobility analyzer to studies of droplet growth or evaporation, *J. Aerosol Sci.*, *17*, 771–787, 1986.

Rader, D., P. McMurry, and S. Smith, Evaporation rates of monodisperse organic aerosols in the 0.02- to 0.2-μm-diameter range, *Aerosol Sci. Technol.*, *6*, 247–260, 1987.

Robinson, A., N. Donahue, M. Shrivastava, E. Weitkamp, A. Sage, A. Grieshop, T. Lane, J. Pierce, and S. Pandis, Rethinking organic aerosols: Semivolatile emissions and photochemical aging, *Science*, *315*, 1259–1262, 2007.

Sakurai, H., K. Park, P. McMurry, D. Zarling, D. Kittelson, and P. Ziemann, Size-dependent mixing characteristics of volatile and nonvolatile components in diesel exhaust aerosol, *Environ. Sci. Technol.*, *37*, 5487–5495, 2003.

Seinfeld, J., and S. Pandis, *Atmospheric chemistry and physics. From air pollution to climate change*, 2nd ed., John Wiley & Sons, Inc., New York, USA, 2006.

Song, C., and G. Carmichael, The aging process of naturally emitted aerosol (sea-salt and mineral aerosol) during long range transport, *Atmos. Environ.*, pp. 2203–2218, 1999.

Stern, J., R. Flagan, D. Grosjean, and J. Seinfeld, Aerosol formation and growth in atmospheric aromatic hydrocarbon photooxidation, *Environ. Sci. Technol.*, *21*, 1224–1231, 1987.

Strommen, M., and R. Kamens, Simulation of semivolatile organic compound microtransport at different time scales in airborne diesel soot particles, *Environ. Sci. Technol.*, *33*, 1738–1746, 1999.

Turpin, B., J. Huntzicker, and S. Hering, Investigation of organic aerosol sampling artifacts in the Los Angeles basin, *Atmos. Environ.*, *28*, 3061–3071, 1994.

Vesterinen, M., K. Lehtinen, M. Kulmala, and A. Laaksonen, Effect of particle phase oligomer formation on aerosol growth, *Atmos. Environ.*, *41*, 1768–1776, 2007.

Wang, J., P. Daum, L. Kleinman, Y.-N. Lee, S. Schwartz, S. Springston, H. Jonsson, D. Covert, and R. Elleman, Observation of ambient aerosol particle growth due to in-cloud processes within boundary layers, *J. Geophys. Res.*, *112*, 14,207, 2007.

Wang, S., and R. Flagan, Scanning electrical mobility spectrometer, *Aerosol Sci. Technol.*, *13*, 230–240, 1990.

Wehner, B., T. Petäjä, M. Boy, C. Engler, W. Birmili, T. Tuch, A. Wiedensohler, and M. Kulmala, The contribution of sulfuric acid and non-volatile compounds on the growth of freshly formed atmospheric aerosols, *Geophys. Res. Lett.*, *32*, L17,810, 2005.

Wiedensohler, A., An approximation of the bipolar charge-distribution for particles in the sub-micron size range, *J. Aerosol Sci.*, *19*, 387–389, 1988.